Quantitation of Chondrocyte Performance in Growth-Plate Cartilage during Longitudinal Bone Growth*

BY ERNST B. HUNZIKER, M.D.†, ROBERT K. SCHENK, M.D.†, AND LUIS-M. CRUZ-ORIVE, PH.D.†, BERNE, SWITZERLAND

From the Institute of Anatomy, University of Berne, Berne

ABSTRACT: **The longitudinal growth of bone depends on the activities of individual chondrocytes of the growth plate. Each chondrocyte remains in a fixed location throughout its life, and there accomplishes all of its functions. Although a cell may perform several or all of its activities simultaneously, one of these will usually predominate during a particular phase of its life. The two most prominent stages are those of cellular proliferation and hypertrophy (including the mineralization of matrix) before the resorption of tissue during vascular invasion.**

By applying recently developed stereological procedures and improved methods for the fixation of cartilage, we compared cellular shape modulation, various ultrastructural parameters (surface areas or volumes of endoplasmic reticulum, Golgi membranes, and mitochondria), the production of matrix, and cellular turnover for proliferating and hypertrophic chondrocytes within the proximal tibial growth plate of the rat.

By the late hypertrophic stage, fourfold and tenfold increases in the mean cellular height and volume, respectively, and a threefold increase in the mean volume of the matrix per cell were achieved. The high metabolic activity of hypertrophic cells was reflected by a twofold to fivefold increase in the mean cellular surface area of rough endoplasmic reticulum, the Golgi membranes, and the mean cellular mitochondrial volume.

Rates of longitudinal growth were determined by fluorochrome labeling and incident-light fluorescence microscopy. Using these values and the stereological estimators describing cellular height, the rates of cellular turnover were calculated. The rapid progression of the vascular invasion front was found to eliminate, for each column of cells, one chondrocyte every three hours; that is, eight cells a day. The maintenance of a steady-state structure for growth-plate cartilage in rats in a steady state of growth thus necessitates efficient compensation for these losses, which is achieved by a high rate of cellular proliferation and rapid hypertrophy.

CLINICAL RELEVANCE: **The development of quantitative histology for bone and its application to the study of biopsy specimens from the human iliac crest have provided valuable new information about metabolic bone diseases which has aided in their diagnosis and treatment. This has become possible only by improvements in stereological methods and procedures for preparing undecalcified sections of bone for histological study. The essential knowledge and methods that are necessary for analogous studies of disorders of growth and of diseases affecting growth-plate cartilage are now available. Although biopsies of the iliac crest and proximal tibial growth plate are performed for diagnostic purposes, only qualitative analyses of sections of tissue have been possible so far. Improved methods of fixation of cartilage that permit the preservation of cellular size, shape, and ultrastructure with minimum distortion, and the development of stereological methods that are designed specifically for application to growth-plate cartilage, now permit quantitative analysis of this tissue and the application of such analysis to the study of disease states.**

Examination of growth-plate cartilage using the light microscope reveals that chondrocytes are organized into layers[5,24,28] (Fig. 1). The similarity in morphological appearance between chondrocytes of a particular zone reflects a synchronization of functional activity between cells that are lateral neighbors. Although a cell may perform several or all of its functions simultaneously, one of these will prevail during a certain period of its life. The dominating activities occur in a defined sequence, and each is initiated and ended by a smooth transition. The morphological characteristics of the principal functional states through which an individual chondrocyte passes during its life in a fixed location are revealed in chronological sequence (that is, from the resting state through proliferation to hypertrophy) within successive zones throughout the growth plate.

It was the purpose of this study to quantitate stereologically and to compare various structural features of chon-

* No benefits in any form have been received or will be received from a commercial party related directly or indirectly to the subject of this article. Funds were received in total or partial support of the research or clinical study presented in this article. The funding source was the Swiss National Science Foundation, Grants 3.148-0.81, 3.058-0.84 (to R. K. S. and E. B. H.), and 3.524-0.83 (to L.-M. C.-O.).

† Institute of Anatomy, University of Berne, Postfach 139, CH-3000 Berne 9, Switzerland.

drocytes (cellular shape modulation, cellular organelles, the production of matrix, and cellular turnover) during the two principal phases of activity: cellular proliferation and hypertrophy. Parameters relating to cellular dimensions and the rate of longitudinal growth were then used to estimate the rate of cellular turnover.

Materials and Methods

Animals

Six female Wistar rats (weighing between 117 and 137 grams), each from a different litter but born on the same day, were injected intraperitoneally with the fluorochrome calceine (Fluka, Buchs, Switzerland) (fifteen milligrams per kilogram of body weight) to permit a determination of their rate of bone growth[24]. They were killed with an overdose of ether five days after injection.

Preparation and Processing of Blocks of Tissue

The diameters of the growth plates (Fig. 3) were measured by a mechanical sliding caliper (Tesa, Switzerland) (accurate to within approximately ten micrometers) for determination of growth-plate reference volumes, calculated by the additional use of the height of the growth plate ($\bar{\tau}$[gpl]) (Table V)[14].

Sagittal slices were cut from the proximal part of the tibia (Fig. 3), and these were transferred to 2 per cent (volume per volume) glutaraldehyde medium, containing 0.7 per cent (weight per volume) ruthenium hexammine trichloride (Johnson-Matthey, England) in 0.05-molar sodium cacodylate buffer (pH 7.4). The slices, which were continually immersed in fixation medium, were additionally dissected into prismatic blocks of tissue under a stereomicroscope. The blocks were maintained in the same fixation solution for two to three hours at 20 degrees Celsius. The blocks were then rinsed in isotonic (osmolarity adjusted with sodium chloride) sodium cacodylate buffer (0.1 molar, pH 7.4) and postfixed in 1 per cent (weight per volume) osmium tetroxide solution in 0.1-molar sodium cacodylate buffer (pH 7.4; osmolarity adjusted to isotonicity with sodium chloride) containing 0.7 per cent (weight per volume) ruthenium hexammine trichloride. Thick (one-micrometer) sections, cut vertically (parallel to the tibial axis) (Fig. 3, *b*), were stained with toluidine blue O, and thin sections were stained with lead citrate and uranyl acetate[30].

The mean thickness of the thick sections was found to be 1.04 micrometer, as determined using a Leitz-Michelson interference phase-contrast microscope for incident light. The thickness of the thin sections was measured by the section-fold method[54] and was found to be thirty-four nanometers. The calibration of magnification for the light microscope was achieved using a Wild stage micrometer and that for the electron microscope, using a Balzers line-grid (2130 lines per millimeter).

Stereology

Determination of the Rate of Longitudinal Bone Growth

A slice of tissue from the proximal part of the tibia of each of the six animals was selected by systematic random sampling (Fig. 3) and fixed in 40 per cent (volume per volume) ethanol for three days. These slices were subsequently dehydrated in ethanol (70, 80, and 95 per cent, and three times 100 per cent [volume per volume]) and embedded in methylmethacrylate that was polymerized at 30 degrees Celsius. Ten-micrometer-thick sagittal sections were cut on a Jung rotary microtome for examination in a Leitz incident-light fluorescence microscope (Fig. 1, *b*). The distances between the zone of vascular invasion within the growth plate and the proximal end-point of the calceine label in the metaphysis were determined using a micrometric eyepiece. Details of this procedure have been described previously[24,25,27,58].

Definitions of Basic Stereological Terms

Stereological estimators always need to be related to a reference volume (space). In the present study, this space was defined either as the sums of the volumes of the left and right proximal tibial growth plates from one animal (V[gpl]) or as the volume of a single stratum (V[str]) such as the zone of proliferating chondrocytes, again for the combined growth plates of a single animal. Within the volume of a particular stratum (V[str]), cells collectively occupy a certain volume (V[c]), and the fraction of this volume that they occupy (V[c]/V[str]) is referred to as the volume density of cells. Cellular surface density (S[c]/V[str]) defines the total cellular surface (S[c]) within the volume of the stratum.

The numerical volume density of cells (N_V = N[c]/V[str]) is the number of cells (N[c]) within the volume of the stratum (V[str]). The number of cellular profiles that are present in the area of the stratum that is exposed on vertical sections through the growth plate is referred to as the numerical area density of cellular profiles (N_A).

The mean horizontal and vertical cellular diameters are symbolized as $\bar{x}$(90 degrees) and $\bar{x}$(zero degrees), respectively.

Histomorphometry

Details of the stereological procedures that were applied in this study have been published elsewhere[14] and are only summarized here.

Two blocks from each leg were chosen by a systematic random-sampling process (Fig. 3). One vertical section per block was cut at random orientation relative to the horizontal plane and was photographed in the light microscope. The boundaries of zones were marked on paper prints (twelve by twenty centimeters), with a final magnification factor of 130 (for the definition of zones, see Figure 1). The volume of the stratum (V[str]) within each growth plate (V[gpl]) was estimated by point-counting, using a test grid that covered the whole section (Fig. 2). The mean vertical thickness of the proliferating zone ($\bar{\tau}$[prl]) was estimated by measuring its thickness at a number of locations on each section (Fig. 2).

The thickness of the other zones (that is, the resting zone, the hypertrophic zone, and the total height of the plate)

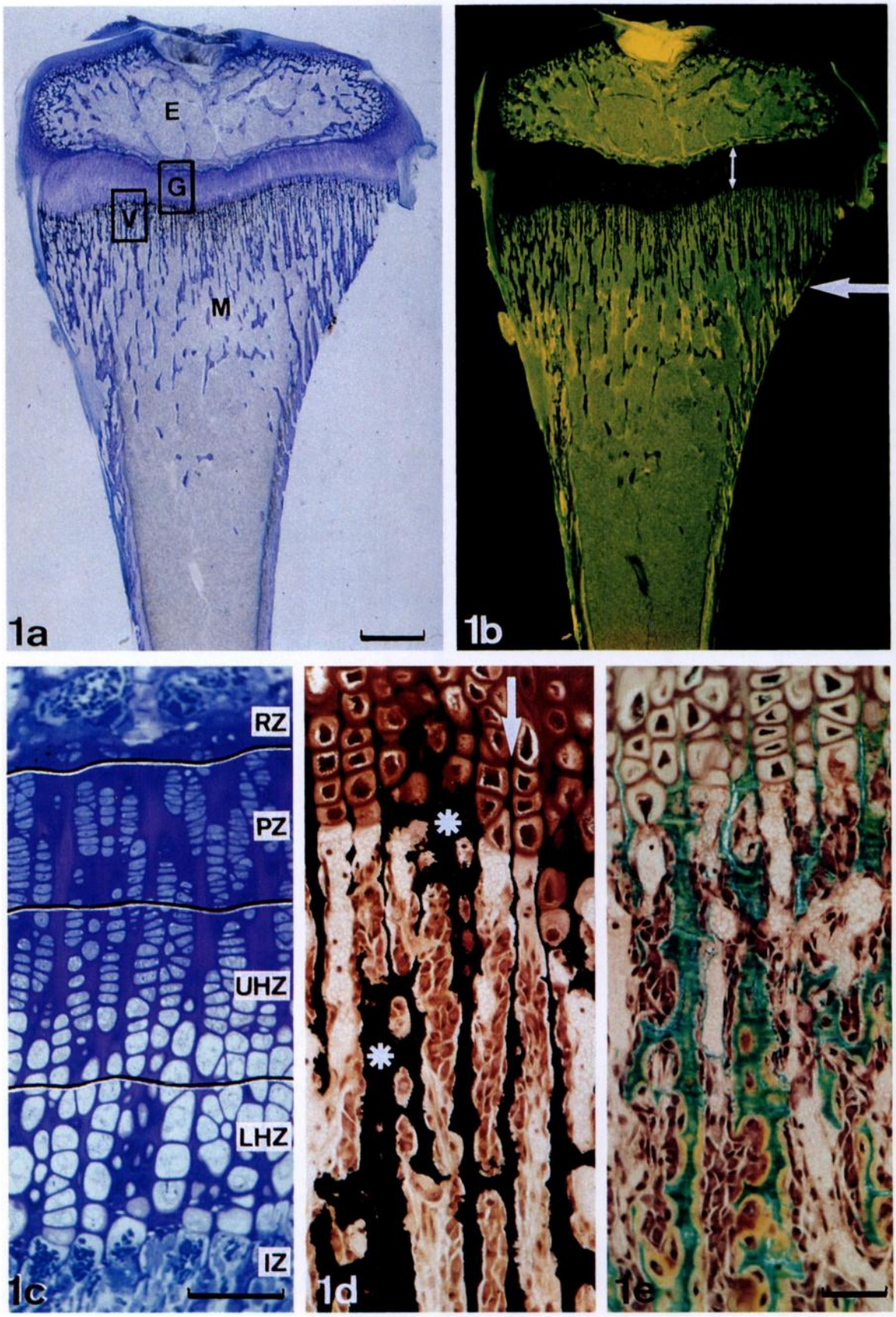

FIG. 1

TABLE I

BASIC STEREOLOGICAL ESTIMATORS OBTAINED FROM LIGHT MICROSCOPIC MEASUREMENTS*

	Reference Volume† V(ref) (mm^3)	Volume Occupied by: Cells V(cells)/V(zone)	Volume Occupied by: Matrix V(matr)/V(zone)	Cellular Surface Area per Unit of Volume S(cells)/V(zone) (cm^2/cm^3)	No. of Cells per Unit of Volume N(cells)/V(zone) ($Cells/mm^3$)
Proliferating zone	9.38 (9.1%)	0.39 (3.0%)	0.61 (3.0%)	1875 (3.3%)	220,500 (5.7%)
Hypertrophic zone‡	10.2 (11.1%)	0.69 (2.0%)	0.31 (2.0%)	1375 (3.3%)	40,700 (7.0%)
Relative change from proliferating to hypertrophic zone	+8.7%	+77%	−49%	−27%	−82%

* The values represent means for six animals. The coefficients of error (calculated among the six animals) are given in parentheses.

† The reference volume (V[ref]) is defined as the sum (union) of the left and right proximal tibial growth plates of an individual animal (for data see Table V).

‡ Refers to the lower half of the hypertrophic zone (for definition see Figure 1, *c*).

was estimated indirectly from the ratios V(str)/V(gpl) and $\bar{\tau}$(prl).

From each section, two quadrants from the proliferating zone and one from the hypertrophic zone (each encompassing the boundaries of the stratum) were subsampled[14,15], photographed, and printed on paper (thirty by forty centimeters), with a final magnification factor of 800. The boundaries of the strata were identified on the basis of those that had been marked on low-magnification prints (magnification factor of 130). However, a more efficient procedure is now available[28].

Within a stratum (V[str]), the total volume of cells (V[c]) was estimated by point-counting (Fig. 4). The total surface area of chondrocytes (S[c]) within a stratum (V[str]) was estimated from vertical sections by intersection-counting using a test system of cycloid test-lines (Fig. 4)[2,14].

Estimation of the total number of chondrocytes (N[c]) within a stratum (V[str]) was achieved using the disector method (Fig. 5)[14,55]. The first and last of five consecutive serial sections (each one micrometer thick) were photographed, and paper prints with a final magnification factor of 800 were prepared. The analysis was facilitated by reference to at least one of the three intermediate sections and by using a test grid (having characteristics such as that shown in Figure 5); the forbidden line rule of Gundersen[21,55] was respected.

The mean sizes of individual cells were estimated using the basic estimators that have already been described[14]: that for mean individual cellular volume ($\bar{v}$[c] = V[c]/N[c]) and that for mean individual cellular surface ($\bar{s}$[c] = S[c]/N[c]). The estimator of the mean cellular equatorial diameter (mean projected horizontal diameter, $\bar{x}$[90 degrees]) of a proliferative chondrocyte was obtained from the relationship: $\bar{x}$(90 degrees) = N_A(90 degrees)/N_V, where N_A(90 degrees) is the numerical profile density per unit of area of the vertical section and N_V is the numerical cellular density per unit of reference volume[14]. An approximate estimate of the mean polar cellular diameter — that is, height ($\bar{x}$[zero degrees]) — was calculated assuming an oblate spheroid model for a proliferative chondrocyte. For hypertrophic chondrocytes, an approximate estimate of the mean cellular equatorial diameter ($\bar{x}$[90 degrees]) was obtained by employing identical methods[14] and an estimate of the mean polar cellular axis ($\bar{x}$[zero degrees]), by modeling cellular shape as a superegg[14].

A basic estimator that is used for calculations of cellular turnover is that of the number of cells ($\bar{n}$[c]) in a column of cells within a given stratum. An approximate value for this estimator was obtained using the following equation: $\bar{n}(c) = \bar{\tau}(str)/\bar{x}(zero\ degrees)$[14].

Fig. 1, *a* through *e*: Photographs and photomicrographs.

a: Frontal section through part of the proximal area of the tibia of the rat, illustrating the epiphyseal bone (E), growth-plate cartilage (G), zone of vascular invasion (V), and metaphysis (M) (toluidine blue O, × 10). The bar indicates one millimeter.

b: Frontal section through part of the proximal area of the tibia of the rat, labeled with calceine and photographed by incident-light fluorescence. Longitudinal growth of bone is measured over a period of five days, as the distance moved by the yellow fluorochrome-label front (horizontal arrow) from the lower border of the growth plate. The height of the growth plate (approximately 580 micrometers) is indicated by the vertical arrow (× 10).

c: High-magnification photomicrograph of the growth plate (see inset G in *a*), fixed in glutaraldehyde containing ruthenium hexammine trichloride[30] (thick [one-micrometer] vertical section, toluidine blue O, × 170). The bar indicates 100 micrometers. The resting zone (RZ) begins immediately under the epiphyseal bone and extends to the upper limit of the proliferating region (PZ). Cells occur singly or in groups of two to a maximum of four, and they are less well oriented with respect to the axis of anisotropy than are those in the other layers. The proliferating zone (PZ) is characterized by flat cells with similar heights (approximately nine micrometers), arranged in distinct columns. The hypertrophic zone (HZ) extends from the lower limit of the proliferating zone to the region of vascular invasion (IZ); it is subdivided, on a purely geometrical basis, into an upper (UHZ) and a lower (LHZ) half. In this investigation, only the lower half (LHZ) was analyzed. Within this region, a mean cellular column consists of approximately five cells, each with a height of approximately thirty-eight micrometers.

d: High-magnification photomicrograph of inset V in *a*, indicating mineralized (stained black) longitudinal septa and metaphyseal bone trabeculae (von Kossa and fuchsin red[49], × 215). The vertical arrow indicates a longitudinal septum cut perpendicularly and the asterisks indicate longitudinal septa cut tangentially.

e: High-magnification photomicrograph of inset V in *a*, stained with Movat-Pentachrome[49] to demonstrate mineralized cartilaginous matrix (blue-green), mineralized bone matrix (yellow), and unmineralized (osteoid) bone matrix (red) (× 215). The bar indicates fifty micrometers.

In *d* and *e*, note the presence of lacunae around shrunken chondrocytes after fixation in ethanol.

TABLE II

ESTIMATED MEAN VALUES OF VARIOUS PARAMETERS FOR INDIVIDUAL CELLS*

	Mean Cellular Volume ($\bar{v}$) (μm^3)	Mean Cellular Surface Area ($\bar{s}$) (μm^2)	Mean Matrix Volume per Cell ($\bar{m}$) (μm^3)	Mean Horizontal Diameter of a Cell ($\bar{x}_d$ [90°]) (μm)	Mean Vertical Diameter (Height) of a Cell ($\bar{x}_d$ [0°]) (μm)
Proliferating zone	1790 (4.7%)	857 (3.1%)	2830 (7.6%)	19.0 (4.3%)	9.6 (6.6%)
Hypertrophic zone	17,400 (6.2%)	3440 (5.4%)	7730 (8.7%)	31.0 (3.6%)	38.5 (5.3%)
Increase factor from proliferating to hypertrophic zone	× 9.7	× 4.0	× 2.7	× 1.6	× 4.0

* Means and coefficients of error (in parentheses) were calculated for six animals.

Electron-Microscopic Stereology

The sampling of blocks was identical to that just described. Sectioning was again restricted to the vertical plane (90 degrees). The sampling of quadrants in the electron microscope was recorded on thirty-five-millimeter film at two primary magnifications: 528 and 7260. Before every sequence of twelve quadrants, a calibration line system was photographed for recording possible fluctuations in magnification[13]. The application of a systematic quadrant-sampling scheme[15,22] throughout each of the two zones usually resulted in a set of eight to twelve quadrants per section. For point-counting and intersection-counting, positive copies of the thirty-five-millimeter negatives were projected on a screen[63], increasing the primary magnification by a factor of ten. Point-counting of nuclei and vacuoles was done at the lower magnification, whereas the measurements of mitochondria, Golgi complexes, and rough endoplasmic reticulum were carried out at higher magnifications.

The numbers of test points and intersections that were counted for each animal and each estimator was in the range of 100 to 200 within each zone (reference space)[22]. The following parameters* were estimated at a final magnification factor of 5280: volume densities of nuclei (V[n]/V[pc], V[n]/V[hc]), vacuoles (V[va]/V[pc], V[va]/V[hc]), and cytoplasm (V[cpl]/V[pc], V[cpl]/V[hc]). At a final magnification factor of 72,600, point-counting and intersection-counting led to the estimation of the volume density and surface density of rough endoplasmic reticulum (V[rER]/V[cpl(pc)], V[rER]/V[cpl(hc)], S[rER]/V[cpl(pc)], S[rER]/V[cpl(hc)]), Golgi apparatus (V[g]/V[cpl(pc)], V[g]/V[cpl(hc)], S[g]/V[cpl(hc)], S[g]/V[cpl(hc)]), and mitochondria (V[m]/V[cpl(pc)], V[m]/V[cpl(hc)]). The absolute quantities of interest were obtained by multiplying the pertinent ratios and the corresponding reference-space volumes.

Data-Processing and Statistics

The morphometric data that were obtained at the light-microscopic level were processed by a Hewlett-Packard 41C calculator, whereas electron-microscopic counting data were first stored in a Hewlett-Packard 9815 microcomputer and later transferred for calculation to a Hewlett-Packard 9830A minicomputer. A general morphometric program that was designed by one of us (L.-M. C.-O.) was then used to calculate the various estimators. Corrections for fluctuations in magnification were integrated[13]. Interblock and interanimal statistics were determined[12,15]. Possible biases due to effects of the thickness or compression of the sections were not corrected for, since they are below the ranges for significant error and cannot be determined reliably.

* N = nuclei, pc = proliferating chondrocytes, hc = hypertrophic chondrocytes, cpl = cytoplasm, va = vacuoles, rER = rough endoplasmic reticulum, g = Golgi apparatus, and m = mitochondria.

Results

Basic Morphology of the Growth Plate of the Rat

Growth plates in the proximal part of tibiae of rats that

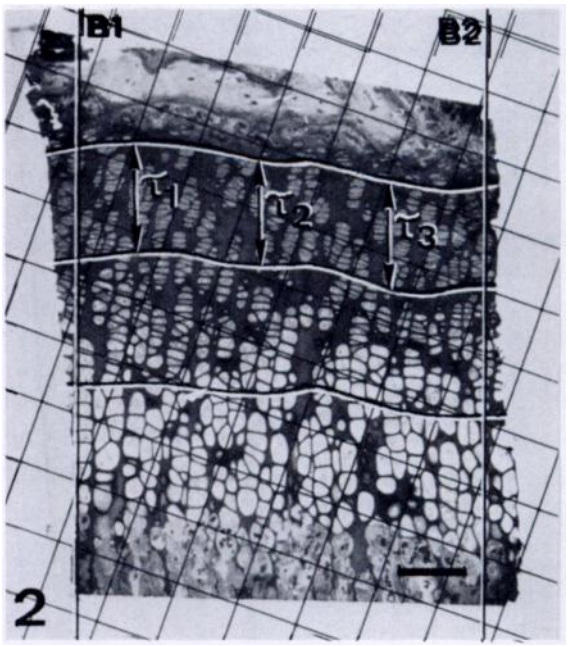

FIG. 2

Light micrograph of a vertical section through the growth-plate cartilage (proximal part of the tibia) (one-micrometer-thick section stained with toluidine blue O, × 85). The bar indicates 100 micrometers.

A test system, superimposed at random on the light micrograph, is used to estimate the mean vertical thickness ($\bar{\tau}$) and volume of each zone. The mean vertical thickness of the proliferating zone is given by the arithmetic mean of the summed measurements τ_1, τ_2, and so on (that is, at points where alternate test lines meet the boundary of the upper zone). The volume ratio between two zones is estimated by the ratio of points counted within the respective zones between the two vertical bars B1 and B2 (to avoid edge effects). Note that the volume ratios of the zones are approximately equal to the corresponding ratios for the mean thickness of the zones.

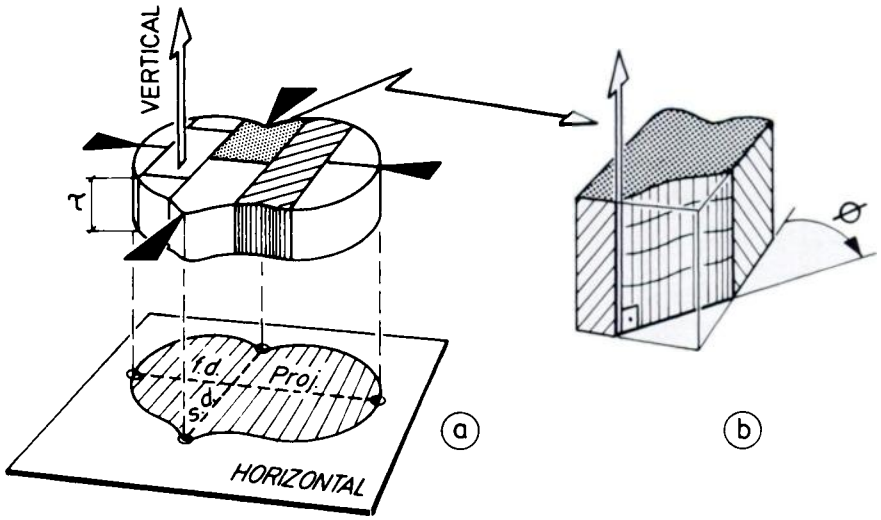

FIG. 3

a: Diagrammatic model of the growth plate. The sagittal and frontal diameters (s.d. and f.d.) must be measured in the intact plate (for instance, at the positions that are marked with arrowheads) in order to estimate its absolute volume[14] (see text). For stereological analysis, two or three blocks per plate are selected at systematically chosen positions that vary from one animal to another. A systematically chosen slice (hatched area in *a*) may be reserved for estimating rates of bone growth.

b: A vertical section from a block, used for estimating the thicknesses of the plate and zone and other stereological quantities pertaining to the matrix, cells, organelles, and so on. Preserving verticality, the section must be cut at an angle ϕ that is randomly chosen between the frontal and sagittal positions, and at a random location within the block.

were in a stage of rapid growth (thirty-five days after birth; mean body weight, approximately 120 grams) were chosen for this investigation. Anatomically, the growth plate appears as an almost flat disk that is interposed between the osseous epiphysis and metaphysis (Fig. 1, *a* and *b*). Histologically, growth-plate cartilage is organized into columns of chondrocytes that parallel the longitudinal axis of the tibia. Various layers are distinguished throughout the height of the growth plate; these are conventionally referred to as the resting, proliferating, and hypertrophic zones (Fig. 1, *c*). In each of these, cells that are lateral neighbors are characterized by a similar phase of activity. During the latter stages of cellular hypertrophy, mineralization of the interterritorial matrix commences and is restricted to the longitudinal septa between columns of cells (Fig. 1, *d*). The pericellular and territorial matrix compartments (Fig. 1, *d* and *e*)[17] within vertical and horizontal septa remain unmineralized and are resorbed at the vascular invasion front together with terminal chondrocytes[32,50].

Not all mineralized longitudinal septa are destined to form primary osseous trabeculae (Fig. 1, *d* and *e*), and indeed about 60 per cent of them are destroyed by the activity of chondroclasts[48,50]. Those that remain are thickened by the deposition of unmineralized bone matrix (osteoid) on the calcified-cartilage matrix core within the metaphysis. The osteoid is subsequently mineralized (from the center outward), and hence the primary spongiosa is laid down (Fig. 1, *e*). By the process of remodeling, this is subsequently replaced by the secondary spongiosa, which consists of cancellous (lamellar) bone.

Stereological Estimators of Growth-Plate Cartilage

Basic parameters that were determined from light-microscopic measurements are given in Table I. The volume density of the chondrocytes in the proliferating zone (the fraction of the total volume of the stratum that is occupied

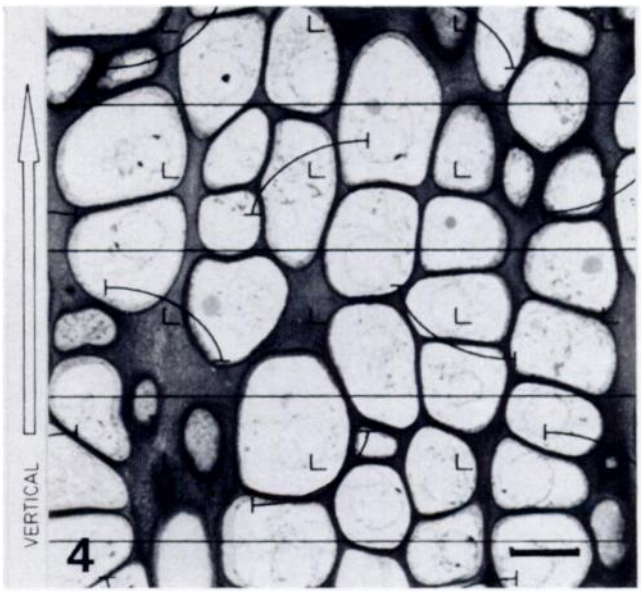

FIG. 4

Light micrograph (× 490) of a vertical section through the hypertrophic zone, superimposed on which is a coherent test system, consisting of test points and test lines (cycloid arcs). The horizontal lines are not used as part of the test system but merely to follow the test arcs easily during counting.

An estimate of cellular volume fractions within the zone is determined as the ratio of the number of test points that fall within the respective compartments; that is, cell or matrix. The cycloid arcs are used for estimating cellular surface area, and it is essential that their vertical axes be aligned with the vertical axis of the section. The cellular surface area is proportional to the number of intersections between cellular profile boundaries and cycloid arcs[2,14]. The bar indicates twenty micrometers.

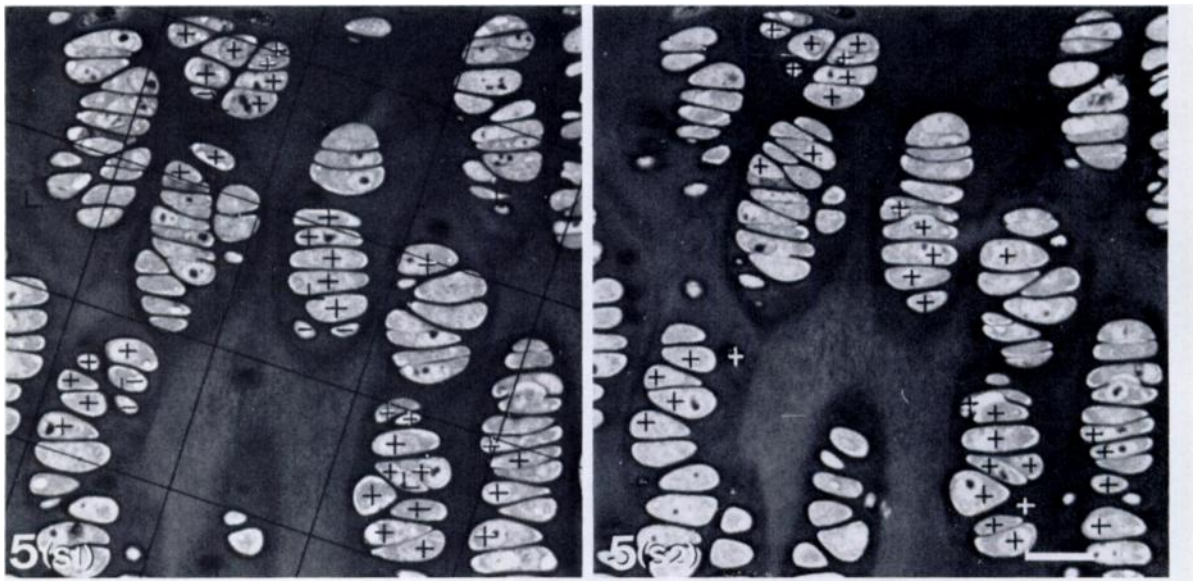

FIG. 5

Counting cells in space using the disector method[14,55]. The upper faces of the two sections that are illustrated (× 510) were cut four micrometers apart in a stack of serial sections. The number of cells that are present in the reference section (S1) but are no longer apparent in the other (S2) (marked with a minus sign), divided by the volume of the disector, gives an estimate of the number of cells per unit of reference volume. Cells that are present in both sections are marked by a plus sign. The disector volume is the product of the reference area (the four squares indicated in S1) and the height of the disector (four micrometers). In each reference square, cellular profiles are selected by the so-called forbidden line unbiased rule of Gundersen[21]. Efficiency can be increased by interchanging the roles of the two sections; that is, regarding S2 rather than S1 as the reference section. The bar indicates twenty micrometers.

by cells) of 0.39 was much lower than the value of 0.69 for that of the chondrocytes of the lower hypertrophic zone (compare data with Fig. 1, *c*), and the relative amounts of cartilaginous matrix that were present in these zones (the volume density of the extracellular matrix) are thus inversely related (0.61 in the proliferating zone compared with 0.31 in the hypertrophic zone). As cellular size increased in the lower hypertrophic zone (Table II), the numerical volume density of these cells (that is, the number of cells per zone volume) decreased considerably (Table I). These results correspond to what would be expected intuitively on light-microscopic examination (Fig. 1).

So-called secondary estimators that were calculated using the basic parameters described in Table I are presented in Table II. These data show that the mean cellular surface in the hypertrophic zone increased by a factor of 4.0 relative to that in the proliferating zone. It should be noted that these estimators relate to light-microscopic measurements; the mean cellular surface ($\bar{s}$) was thus equivalent to the mean surface of the lacunar wall and did not represent an exact surface area of the plasmalemma.

It is apparent from Table II that the mean cellular volume increased considerably (by a factor of approximately ten), a change during hypertrophy that occurred concomitantly with an increase in cellular height (by a factor of approximately four). These massive (and rapid) changes in cellular dimensions gave the hypertrophic cells the appearance of being water-rich (and electrolyte-rich) cells that had a low density of organelles (Fig. 6).

The low volume density that was occupied by matrix within the hypertrophic zone (0.31) and its tenuous appearance around the cells (Fig. 1, *c*) gave a deceptive impression of its actual volume in relation to individual cells. Calculation of this parameter revealed that the hypertrophic cells actually increased their individual (average) matrix volume by a factor of approximately three compared with the cells in the proliferating zone (Table II).

The visual impression of low organellar density within the hypertrophic cells (Fig. 6, *b*) was confirmed by the quantitative data (Table III). This impression is accentuated when the data are compared with those for proliferating chondrocytes (Table III and Fig. 6, *a*).

The absolute volumes and surface areas of the organelles that were involved in the production of matrix and cellular growth were estimated quantitatively (Table IV). A comparison between individual chondrocytes within the two zones revealed an absolute increase by a factor of between 2.5 and five in both parameters on passing from the proliferating to the hypertrophic zone.

Determinations of longitudinal growth by incident-light fluorescence microscopy (Fig. 1, *b*) were carried out on each epiphyseal plate, and the mean value was calculated for each animal. The mean rate of growth in length of the proximal part of the tibia for all animals was found to be 330 micrometers a day, as measured during the last five days before the rats were killed.

Estimations of daily rates of cellular turnover were obtained by dividing the average longitudinal growth per day by the mean height of a (lower) hypertrophic cell (Table II). It was found that approximately eight chondrocytes need to be eliminated and replaced each day; that is, on average, one chondrocyte (including its complete unmineralized-matrix coat) every three hours. The mean values for the heights of the zones are presented in Table V. On the basis of these

TABLE III

MEAN RELATIVE AND ABSOLUTE VOLUMES AND SURFACE AREAS* OF ORGANELLES IN ALL OF THE CELLS FROM PROXIMAL TIBIAL GROWTH PLATES†

	Rough Endoplasmic Reticulum				Golgi Apparatus				Mitochondria		Nuclei		Vacuoles	
	Volume		Surface Area		Volume		Surface Area		Volume		Volume		Volume	
	V(rER)/ V(cpl)	V(rER) (mm^3)	S(rER)/ V(cpl) (cm^{-1})	S(rER) (cm^2)	V(g)/ V(cpl)	V(g) (mm^3)	S(g)/ V(cpl) (cm^{-1})	S(g) (cm^2)	V(m)/ V(cpl)	V(m) (mm^3)	V(n)/ V(cell)	V(n) (mm^3)	V(v)/ V(cell)	V(v) (mm^3)
Proliferating zone	0.19 (4%)	0.58 (10.5%)	30,700 (2.7%)	93.2 (10.1%)	0.08 (10.8%)	0.24 (14.5%)	4558 (5.9%)	13.8 (11.3%)	0.026 (3.4%)	0.08 (10.3%)	0.17 (1.7%)	0.62 (9.7%)	0.12 (17.3%)	0.44 (19.7%)
Hypertrophic zone	0.05 (6.4%)	0.29 (13.1%)	8120 (4.5%)	47.2 (12.4%)	0.03 (7.2%)	0.19 (13.6%)	2134 (9.4%)	12.4 (14.8%)	0.009 (11.1%)	0.05 (16%)	0.17 (2.3%)	1.2 (11.5%)	0.26 (3.9%)	1.82 (11.9%)
Relative change from proliferating to hypertrophic zone	−74%	−50%	−74%	−49%	−63%	−21%	−53%	−10%	−65%	−38%	0%	+94%	+117%	+314%

* The values represent means for six animals. The coefficients of error (calculated among the six animals) are given in parentheses.

† The absolute volumes (mm^3) and surface areas (cm^2) pertain to the reference space (V[ref]), representing the sum (union) of the left and right proximal tibial growth plates of an animal (for data see Table V). The reference compartments in this table are either total cell cytoplasm (cpl) or total cell (cell) in the growth plates.

results and the mean rates of cellular turnover, it was calculated that the activity phase for a cell of the lower hypertrophic zone has a mean duration of approximately fifteen hours.

Discussion

During its life, an epiphyseal chondrocyte passes through various phases, each of which is characterized by a predominating functional activity. These phases occur in synchrony for chondrocytes of similar ages; hence, on passing through the growth plate from the youngest, proliferating cells to the oldest ones in the region of vascular invasion, the life history of an individual chondrocyte is re-enacted.

Changes in the Size and Shape of Chondrocytes

During hypertrophy, cellular volume and height were found to increase by factors of approximately ten and four, respectively (Table II), thus contributing significantly to the longitudinal growth of bone.

While the stereological estimates of mean cellular volume and surface area are independent of assumptions for shape, the estimators of cellular dimensions in both zones were derived using a prolate spheroid model for a proliferating cell and a superegg model (obtained geometrically by revolving a super ellipse) for a chondrocyte in the late hypertrophic stage[14]. The model for proliferating chondrocytes tends to overestimate their height, since it assumes convex curvature of the top and bottom areas; in reality, flat and even concave profiles may also appear (Figs. 1, *c*; 2; and 6, *a*). A more appropriate model for these calculations is not available, however. A consequence of this bias of the model is that the absolute increase in cellular height that is attained during transition to the hypertrophic phase is probably greater than a factor of four (Table II).

Individual cellular height increases continuously throughout the hypertrophic phase, but visual examination of tissue shows that the rate at which this occurs will vary somewhat among cells. Hence, although there is an overall increase in cellular height along a column of cells in the lower hypertrophic zone, the change is not a smooth one. As a result of this trend, the mean cellular height that is calculated for this zone will tend to underestimate the final

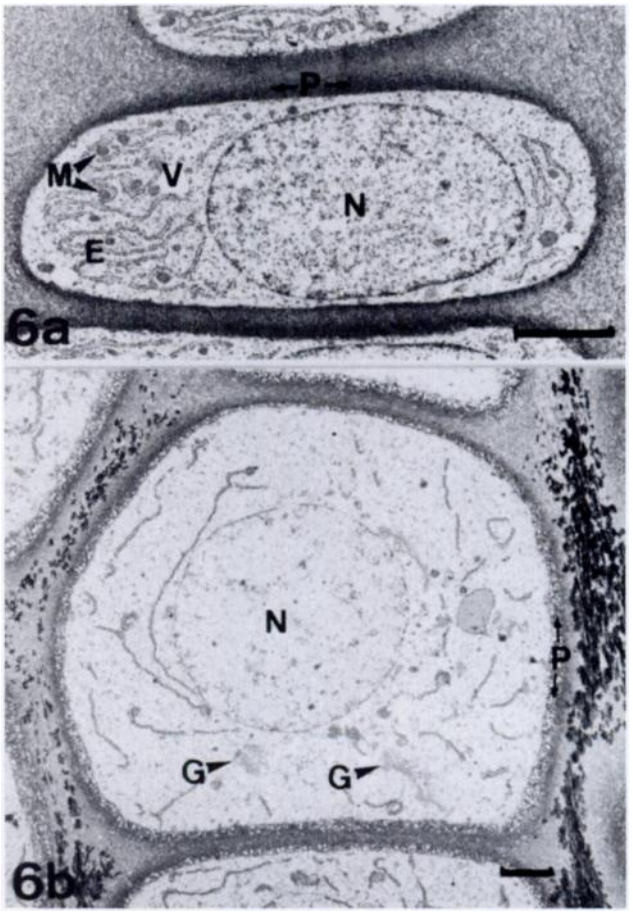

FIG. 6

Electron micrographs of a proliferating (*a*) and a hypertrophic (*b*) chondrocyte. Both cells are preserved in an expanded state, with their plasmalemmata in intimate contact with the pericellular matrix after fixation with ruthenium hexammine trichloride. The magnification of *a* (× 4300) is approximately twice that of *b* (× 2200). Each bar indicates three micrometers. N = nucleus, M = mitochondrion, E = rough endoplasmic reticulum, G = Golgi area, V = vacuoles, and P = pericellular matrix.

TABLE IV

ESTIMATED MEAN SURFACE AREAS AND VOLUMES OF ORGANELLES IN AN INDIVIDUAL CELL IN THE PROLIFERATING AND HYPERTROPHIC ZONES*

	Volume Occupied by rER in a Cell ($\bar{v}$[rER]) (μm^3)	Surface Area of rER in a Cell ($\bar{s}$[rER]) (μm^2)	Volume Occupied by Golgi Apparatus in a Cell ($\bar{v}$[g]) (μm^3)	Surface Area of Golgi Membranes in a Cell ($\bar{s}$[g]) (μm^2)	Volume Occupied by Mitochondria in a Cell $\bar{v}$(m) (μm^3)	Volume Occupied by Vacuoles in a Cell $\bar{v}$(va) (μm^3)
Proliferating zone	284 (5.5%)	4500 (4.0%)	112 (9.6%)	668 (4.4%)	39 (5.4%)	190 (15.0%)
Hypertrophic zone	700 (9.8%)	11,800 (8.9%)	480 (12.6%)	3132 (13.4%)	129 (11.3%)	4490 (8.2%)
Increase factor per cell	× 2.5	× 2.6	× 4.3	× 4.7	× 3.3	× 24

* The values represent means for six animals. The coefficients of error (calculated among the six animals) are given in parentheses.

increase in height that is achieved by an individual cell.

Activity of the Chondrocytes

Considering that matrix proteoglycans are present at very high concentrations and that the intrinsic pressure in the cartilaginous matrix is on the order of two to three atmospheres[42,43,60], it seems reasonable to assume that the chondrocytes achieve their increase in volume by active transportation of fluid (water and electrolytes) across the plasmalemma into the intracellular space[7,19,36,39,47]. This view is supported by the finding that the absolute mitochondrial mass per cell increases by a factor of 3.3 (Table III) during this phase[10,45]. Moreover, this increase in the absolute mitochondrial mass probably only partially reflects the increase in metabolic activity since, during hypertrophy, chondrocytes gain energy additionally by means of the glycolytic pathway[3,9,26]. The decrease in the number of cells of 80 per cent that was found per unit of volume of tissue (Table I) is not a surprising phenomenon in view of the tremendous increase in volume (Table II) that occurs during this transition.

Changes in the Matrix

On visual inspection of the growth plate, there was a relative decrease in the proportion of matrix per cellular profile in passing from the proliferating to the hypertrophic zone (from 0.61 to 0.31) (Table I), and one can be misled into believing that massive degradation of this material must have taken place[4,24,57]. However, examination of the mean absolute volume of matrix per cell reveals an actual increase in this parameter by a factor of approximately three on passing from the proliferating to the final hypertrophic state (Table II). Due to the high internal pressure within the cartilage, it is extremely unlikely that the increased volume of the matrix is attributable to increased hydration exclusively within one zone. The increase in the production of matrix additionally supports the view that cells in the late hypertrophic phase must have a rapid metabolic turnover[16,23,46,56,61]. Figure 7 illustrates the mean quantitative changes in individual cellular and matrix volume that are produced at this stage; the model is represented on three-dimensional grounds and in correct numerical proportions to the quantitative estimators of Table II. The transformation in cellular size and shape is accompanied not only by an increase in the production of matrix but also by extensive remodeling of this material[6,59] in order to adapt to the changes in cellular size and morphology. Furthermore, the production of matrix is probably not restricted merely to covering the needs of the increased spatial domain around the individual cell (as illustrated in Figure 7), since the extensive structural rearrangement of the chondrocyte probably necessitates at least partial degradation of matrix[18,61], which then has to be resynthesized. Hence, the actual amount of matrix that is synthesized during remodeling will be higher than the net increase in volume that is measured. Despite the extent of remodeling of the matrix that occurs during the transformation of cellular shape, the highly ordered structure within the various compartments (pericellular, territorial, and interterritorial) is maintained[17]. Precisely how the degradative and synthetic processes are coordinated to maintain these topographical relationships is, however, not understood.

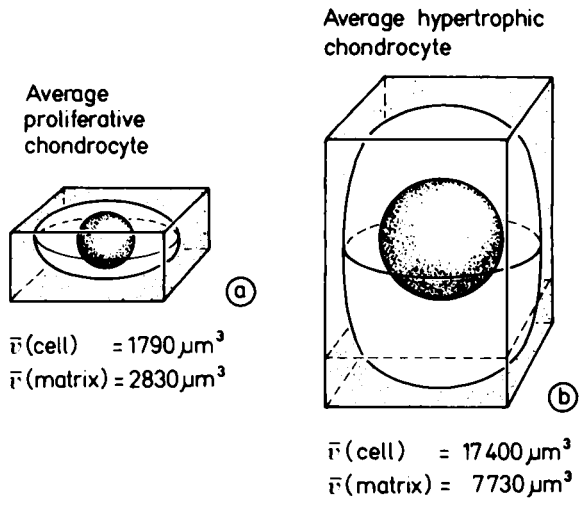

FIG. 7

Three-dimensional representation of the increases in matrix (approximately threefold), cellular volume (approximately tenfold), and height (approximately fourfold) that are achieved on transition from the proliferating (*a*) to the hypertrophic (*b*) phase. The volume of dense dots around the cells represents the mean matrix volume surrounding a proliferating chondrocyte. The volume of sparser dots represents the newly formed matrix around a hypertrophic chondrocyte. This value represents the minimum increase in volume and does not include the contribution from newly formed matrix that was degraded as part of the process of remodeling. The combined volumes (dense dots and sparse dots) represent the final volume of matrix surrounding a hypertrophic cell.

TABLE V

MEAN HEIGHT AND VOLUME OF A WHOLE GROWTH PLATE AND OF INDIVIDUAL ZONES*

	Total Growth Plate	Resting Zone	Proliferating Zone	Hypertrophic Zone	
				Upper	Lower
Height (μm)	583 (8.1%)	42 (8.8%)	171 (5.0%)	185 (8.1%)	185 (8.1%)
Volume (mm^3)	16.0 (7.6%)	1.15 (10.1%)	4.69 (7.1%)	5.08 (10.7%)	5.08 (10.7%)

* Means for six animals. The coefficients of error (calculated among the six animals) are given in parentheses.

Cytoplasmic Organelles

A visual assessment of the quantitative relationships among the cytoplasmic organelles that are involved in cellular activity (such as Golgi apparatus, rough endoplasmic reticulum [rER], and mitochondria) in proliferating (Fig. 6, *a*) and hypertrophic (Fig. 6, *b*) chondrocytes suggests that there is a reduction in this activity during the hypertrophic phase, and the morphometric data relating to these parameters (Table III) confirm that impression. The relative reduction in the density of the organelles is, however, a consequence of the increase in cellular volume, since within an individual cell the absolute amounts of these cytoplasmic organelles actually increase by a factor of between 2.5 and five (Table IV). These data again support the view that hypertrophic chondrocytes are metabolically very active[32].

Although, in several previous reports, hypertrophic chondrocytes have been described as being active on the basis of measurements relating to the synthesis of protein[20,40,46,51,52], the enzyme content[1,37], the synthesis of ribonucleic acid[41], and the incorporation of ^{35}S[8,38,53], in those reports the definition of the hypertrophic zone excluded the region that is described as the lower hypertrophic zone in our study. For this reason, too, a previous morphometric analysis of cellular parameters and organelles within the so-called hypertrophic zone[5] is not compatible with ours. Furthermore, that investigation[5], not being a stereological (three-dimensional), assumption-free study, remained restricted to the two-dimensional plane.

Tissue and Cellular Morphology

Until cryotechnical techniques of processing were applied to cartilaginous tissue[32], the term hypertrophic cell referred exclusively to chondrocytes within the region that is defined as the upper hypertrophic zone in this report; the five to six layers of cells that are here designated as the lower hypertrophic zone were previously defined as degenerating and mineralizing[4,24,57]. This older definition was based on histological examination of tissue that was fixed using conventional chemical techniques. Under these conditions, cells in the late hypertrophic phase are particularly susceptible to shrinkage and plasmalemmal rupture[31]. The loss of proteoglycans from the extracellular matrix surrounding cells in this region also appears to be considerable, and leads to the formation of lacunae[29,31]. The use of cryotechnical methods of tissue-processing has led to a new view of the function of chondrocytes in the late hypertrophic phase[32]. Chondrocytes within the so-called degenerating zone, and indeed in all zones throughout the entire epiphyseal plate, were found to be morphologically intact. They were found to be in intimate contact with the pericellular matrix, and there was no formation of lacunae. The space surrounding the cell in chemically fixed tissue was believed to be an artefact[30-32]. Hypertrophy thus appears as a continuous process up to the point of metaphyseal blood-vessel ingrowth, where the mineralization of matrix begins to take place. Our definition of the hypertrophic zone therefore includes the previously defined mineralizing and degenerating regions (that is, the final five or six chondrocytes above the ingrowing vessels) (Figs. 1, *c*; 4; and 6, *b*).

Chemical fixation in the presence of ruthenium hexammine trichloride (as used in this investigation) has also been found to overcome the problems of the preservation of cellular shape and the formation of lacunae[29-31]. The results of this investigation confirm that cells in the lower hypertrophic zone are intact not only morphologically[32] but also functionally, and that metabolically they are very active[11,44,64].

A disadvantage that is associated with all chemical techniques of fixation, however, is the occurrence of intracellular vacuoles[24,30]. These artefacts are particularly apparent when a cationic dye has been used, such as ruthenium hexammine trichloride, which causes the precipitation of proteoglycans with consequent shrinkage of the extracellular matrix. Since ruthenium hexammine trichloride also acts by strengthening the interaction between components of the cellular membrane and proteoglycans within the pericellular matrix[31], the cellular membrane will remain adherent to these proteoglycans during shrinkage of the matrix, resulting in a compensatory increase in cellular volume producing the formation of vacuoles[30] (Fig. 6, *a*). According to this proposed effect of ruthenium hexammine trichloride, the total volume of vacuoles per cell would be expected to increase as a function of changes in cellular and matrix volume. It is interesting in this respect that the total increase in the formation of vacuoles (approximately twenty-four times) is almost identical to the combined increase in cellular and matrix volume (approximately twenty-six times) on passing from the proliferating to the hypertrophic zone.

Cellular and Matrix Turnover

The processes of cellular transformation and remodeling of the matrix occur quite quickly. The rapid vascular ingrowth (approximately 0.3 millimeter in twenty-four hours) that occurs in rats of this age-group leads to the elimination of one hypertrophic chondrocyte, including its matrix coat (pericellular and territorial zones), every three

hours; that is, approximately eight chondrocytes are eliminated and replaced every day for each column of cells. Assuming steady-state conditions of turnover for growth-plate chondrocytes, the time that is required for an individual cell to complete hypertrophy may be calculated using estimators of the cellular height, the height of the zone, and the rate of cellular elimination. This calculation reveals that the late hypertrophic phase is completed within twelve to fifteen hours.

Previous estimations of rates of cellular turnover using labeling with ^{3}H-thymidine gave slightly different results[33,34,62]; the differences may be due mainly to differences in the estimated cellular height[34,35,57]. In earlier studies, this parameter was measured in the two-dimensional plane and thus represented the cellular profile height, whereas in the current investigation the estimations were based on a three-dimensional model.

The data that were gained from this investigation have permitted characterization of the performance of chondrocytes during endochondral growth on a quantitative basis. In particular, data relating to cells in the late stage of hypertrophy revealed that they are metabolically very active even during this final phase of the process, thus confirming previous morphological findings that these cells are structurally intact[32]. It is hoped that the information that was obtained from this investigation not only will help to improve our understanding of the physiology of the growth plate but also will serve as a basis on which to assess the influence of drugs or altered endocrine functions on the longitudinal growth of bone.

NOTE: The authors thank Ceri England for the English correction of the manuscript, Fritz Ruch for the use of his Leitz-Michelson interference phase-contrast microscope and his help, Wolfgang Herrmann for the skillful production of the illustrations and the photographic work, Werner Graber for performing the morphometric measurements, and Markus Baumgartner for programming the computers.

References

1. AKISAKA, T.: The Localization of Thiamine Pyrophosphatase Activity in Meckel's Cartilage Cells during Endochondral Ossification. Histochemistry, **76:** 539-546, 1982.
2. BADDELEY, A. J.; GUNDERSEN, H. J. G.; and CRUZ-ORIVE, L. M.: Estimation of Surface Area from Vertical Sections. J. Microsc., **142:** 259-276, 1986.
3. BORLE, A. B.; NICHOLS, NANCY; and NICHOLS, GEORGE, JR.: Metabolic Studies of Bone in Vitro. I. Normal Bone. J. Biol. Chem., **235:** 1206-1210, 1960.
4. BRIGHTON, C. T.: Structure and Function of the Growth Plate. Clin. Orthop., **136:** 22-32, 1978.
5. BRIGHTON, C. T.; SUGIOKA, YOICHI; and HUNT, R. M.: Cytoplasmic Structures of Epiphyseal Plate Chondrocytes. Quantitative Evaluation Using Electron Micrographs of Rat Costochondral Junctions with Special Reference to the Fate of Hypertrophic Cells. J. Bone and Joint Surg., **55-A:** 771-784, June 1973.
6. BRUNS, R. R.; HULMES, D. J. S.; THERRIEN, S. F.; and GROSS, JEROME: Procollagen Segment-Long-Spacing Crystallites. Their Role in Collagen Fibrillogenesis. Proc. Nat. Acad. Sci., **76:** 313-317, 1979.
7. BUCKWALTER, J. A.; MOWER, DONALD; UNGAR, ROBIN; SCHAEFFER, JANICE; and GINSBERG, BARRY: Morphometric Analysis of Chondrocyte Hypertrophy. J. Bone and Joint Surg., **68-A:** 243-255, Feb. 1986.
8. CAMPO, R. D., and DZIEWIATKOWSKI, D. D.: Turnover of the Organic Matrix of Cartilage and Bone as Visualized by Autoradiography. J. Cell Biol., **18:** 19-29, 1963.
9. COHN, D. V., and FORSCHER, B. K.: Aerobic Metabolism of Glucose by Bone. J. Biol. Chem., **237:** 615-618, 1962.
10. COPE, G. H.: Exocrine Glands and Protein Secretion. A Stereological Viewpoint. J. Microsc., **131:** 187-202, 1983.
11. CRELIN, E. S., and KOCH, W. E.: An Autoradiographic Study of Chondrocyte Transformation into Chondroclasts and Osteocytes during Bone Formation in Vitro. Anat. Rec., **158:** 473-484, 1967.
12. CRUZ-ORIVE, L. M.: Best Linear Unbiased Estimators for Stereology. Biometrics, **36:** 595-605, 1980.
13. CRUZ-ORIVE, L. M.: The Use of Quadrats and Test Systems in Stereology, Including Magnification Corrections. J. Microsc., **125:** 89-102, 1982.
14. CRUZ-ORIVE, L. M., and HUNZIKER, E. B.: Stereology for Anisotropic Cells: Application to Growth Cartilage. J. Microsc., **143:** 47-80, 1986.
15. CRUZ-ORIVE, L. M., and WEIBEL, E. R.: Sampling Designs for Stereology. J. Microsc., **122:** 235-257, 1981.
16. DINGLE, J. T., and DINGLE, T. T.: The Site of Cartilage Matrix Degradation. Biochem. J., **190:** 431-438, 1980.
17. EGGLI, P. S.; HERRMANN, WOLFGANG; HUNZIKER, E. B.; and SCHENK, R. K.: Matrix Compartments in the Growth Plate of the Proximal Tibia of Rats. Anat. Rec., **211:** 246-257, 1985.
18. EHRLICH, M. G.; ARMSTRONG, A. L.; NEUMAN, R. G.; DAVIS, M. W.; and MANKIN, H. J.: Patterns of Proteoglycan Degradation by a Neutral Protease from Human Growth-Plate Epiphyseal Cartilage. J. Bone and Joint Surg., **64-A:** 1350-1354, Dec. 1982.
19. GOULD, G. W., and MEASURES, J. C.: Water Relations in Single Cells. Philos. Trans. Roy. Soc. Lond. [Biol.], **278:** 151-166, 1977.
20. GRANT, W. T.; SUSSMAN, M. D.; and BALIAN, GARY: A Disulfide-Bonded Short Chain Collagen Synthesized by Degenerative and Calcifying Zones of Bovine Growth Plate Cartilage. J. Biol. Chem., **260:** 3798-3803, 1985.
21. GUNDERSEN, H. J. G.: Notes on the Estimation of the Numerical Density of Arbitrary Profiles: The Edge Effect. J. Microsc., **111:** 219-223, 1977.
22. GUNDERSEN, H. J. G.: Stereology and Sampling of Biological Surfaces. *In* Analysis of Organic and Biological Surfaces, pp. 477-506. Edited by Patrick Echlin. New York, Wiley, 1984.
23. HANDLEY, C. J.; SPEIGHT, G.; LEYDEN, K. M.; and LOWTHER, D. A.: Extracellular Matrix Metabolism by Chondrocytes. 7. Evidence that L-Glutamine Is an Essential Amino Acid for Chondrocytes and Other Connective Tissue Cells. Biochim. Biophys. Acta, **627:** 324-331, 1980.
24. HANSSON, L. I.: Daily Growth in Length of Diaphysis Measured by Oxytetracycline in Rabbit Normally and after Medullary Plugging. Acta Orthop. Scandinavica, Supplementum 101, 1967.
25. HANSSON, L. I.; MENANDER-SELLMAN, K.; STENSTRÖM, A.; and THORNGREN, K.-G.: Rate of Normal Longitudinal Bone Growth in the Rat. Calcif. Tissue Res., **10:** 238-251, 1972.
26. HOUGH, STEPHEN; RUSSELL, J. E.; TEITELBAUM, S. L.; and AVIOLI, L. V.: Regulation of Epiphyseal Cartilage Metabolism and Morphology in the Chronic Diabetic Rat. Calcif. Tissue Internat., **35:** 115-121, 1983.
27. HULTH, A., and OLERUD, S.: Tetracycline Labelling of Growing Bone. Acta Soc. Med. Upsaliensis, **67:** 219-231, 1962.
28. HUNZIKER, E. B., and CRUZ-ORIVE, L. M.: Consistent and Efficient Delineation of Reference Spaces for Light Microscopical Stereology Using a Laser Microbeam System. J. Microsc., **142:** 95-99, 1986.
29. HUNZIKER, E. B., and SCHENK, R. K.: Structural Organization of Proteoglycans in Cartilage. *In* Biology of Proteoglycans. Edited by T. N. Wight and R. P. Mecham. New York, Academic Press, in press.
30. HUNZIKER, E. B.; HERRMANN, W.; and SCHENK, R. K.: Improved Cartilage Fixation by Ruthenium Hexammine Trichloride (RHT). A Prerequisite for Morphometry in Growth Cartilage. J. Ultrastruct. Res., **81:** 1-12, 1982.
31. HUNZIKER, E. B.; HERRMANN, WOLFGANG; and SCHENK, R. K.: Ruthenium Hexammine Trichloride (RHT)-Mediated Interaction between Plasmalemmal Components and Pericellular Matrix Proteoglycans Is Responsible for the Preservation of Chondrocytic Plasma Membranes in Situ during Cartilage Fixation. J. Histochem. and Cytochem., **31:** 717-727, 1983.
32. HUNZIKER, E. B.; HERRMANN, W.; SCHENK, R. K.; MUELLER, M.; and MOOR, H.: Cartilage Ultrastructure after High Pressure Freezing, Freeze Substitution, and Low Temperature Embedding. I. Chondrocyte Ultrastructure. Implications for the Theories of Mineralization and Vascular Invasion. J. Cell Biol., **98:** 267-276, 1984.

33. KEMBER, N. F.: Cell Division in Endochondral Ossification. A Study of Cell Proliferation in Rat Bones by the Method of Tritiated Thymidine Autoradiography. J. Bone and Joint Surg., **42-B(4):** 824-839, 1960.
34. KEMBER, N. F.: Cell Kinetics of Cartilage. *In* Cartilage, edited by B. K. Hall. Vol. 1, pp. 149. New York, Academic Press, 1983.
35. KEMBER, N. F., and WALKER, K. V. R.: Control of Bone Growth in Rats. Nature, **229:** 428-429, 1971.
36. KREGENOW, F. M.: Osmoregulatory Salt Transporting Mechanisms. Control of Cell Volume in Anisotonic Media. Ann. Rev. Physiol., **43:** 493-505, 1981.
37. KUHLMAN, R. E., and MCNAMEE, M. J.: The Biochemical Importance of the Hypertrophic Cartilage Cell Area to Enchondral Bone Formation. J. Bone and Joint Surg., **52-A:** 1025-1032, July 1970.
38. KUNIN, A. S., and KRANE, S. M.: The Effect of Dietary Phosphorus on the Intermediary Metabolism of Epiphyseal Cartilage from Rachitic Rats. Biochim. Biophys. Acta, **107:** 203-214, 1965.
39. MACKNIGHT, A. D. C., and LEAF, ALEXANDER: Regulation of Cellular Volume. Physiol. Rev., **57:** 510-573, 1977.
40. MANKIN, H. J., and LIPPIELLO, LOUIS: Nucleic Acid and Protein Synthesis in Epiphyseal Plates of Rachitic Rats. An Autoradiographic Study. J. Bone and Joint Surg., **51-A:** 862-874, July 1969.
41. MANKIN, H. J.; REVAK, CONRAD; and LIPPIELLO, LOUIS: Ribonucleic Acid Synthesis in the Epiphyseal Plate of the Rat. An Autoradiographic Study. Bull. Hosp. Joint Dis., **29:** 111-119, 1968.
42. MAROUDAS, A.: Transport through Articular Cartilage and Some Physiological Implications. *In* Symposium on Normal and Osteoarthrotic Articular Cartilage, edited by S. Y. Ali, M. W. Elves, and D. H. Leaback. Proceedings, p. 33. London, University of London, 1973.
43. MAROUDAS, A., and BANNON, C.: Measurement of Swelling Pressure in Cartilage and Comparison with the Osmotic Pressure of Constituent Proteoglycans. Biorheology, **18:** 619-632, 1981.
44. MATUKAS, V. J.; PANNER, B. J.; and ORBISON, J. L.: Studies on Ultrastructural Identification and Distribution of Protein-Polysaccharide in Cartilage Matrix. J. Cell Biol., **32:** 365-377, 1967.
45. NOMURA, MASAYASU: The Control of Ribosome Synthesis. Scient. Am., **250:** 102-114, 1984.
46. OOHIRA, ATSUHIKO; KIMATA, KOJI; SUZUKI, SAKARU; TAKATA, KENZO; SUZUKI, IKUO; and HOSHINO, MUNEMITSU: A Correlation between Synthetic Activities for Matrix Macromolecules and Specific Stages of Cytodifferentiation in Developing Cartilage. J. Biol. Chem., **249:** 1637-1645, 1974.
47. REITH, E. J.: A Model for Transcellular Transport of Calcium Based on Membrane Fluidity and Movement of Calcium Carriers within the More Fluid Microdomains of the Plasma Membrane. Calcif. Tissue Internat., **35:** 129-134, 1983.
48. SCHENK, R. K.: Basic Histomorphology and Physiology of Skeletal Growth. *In* Treatment of Fractures in Children and Adolescents, pp. 3-19. Edited by B. G. Weber, C. Brunner, and F. Freuler. Berlin, Springer, 1980.
49. SCHENK, R. K.; OLAH, A. J.; and HERRMANN, W.: Preparation of Calcified Tissues for Light Microscopy. *In* Methods of Calcified Tissue Preparation, p. 1. Edited by G. R. Dickson. New York, Elsevier, 1984.
50. SCHENK, R. K.; SPIRO, DAVID; and WIENER, JOSEPH: Cartilage Resorption in the Tibial Epiphyseal Plate of Growing Rats. J. Cell Biol., **34:** 275-291, 1967.
51. SCHMID, T. M., and CONRAD, H. E.: Metabolism of Low Molecular Weight Collagen by Chondrocytes Obtained from Histologically Distinct Zones of the Chick Embryo Tibiotarsus. J. Biol. Chem., **257:** 12451-12457, 1982.
52. SCHMID, T. M., and LINSENMAYER, T. F.: Developmental Acquisition of Type X Collagen in the Embryonic Chick Tibiotarsus. Devel. Biol., **107:** 373-381, 1985.
53. SEINSHEIMER, FRANK, and SLEDGE, C. B.: Parameters of Longitudinal Growth Rate in Rabbit Epiphyseal Growth Plates. J. Bone and Joint Surg., **63-A:** 627-630, April 1981.
54. SMALL, J. V.: Measurements of Section Thickness. *In* Proceedings of the Fourth European Regional Conference on Electron Microscopy, edited by D. S. Bocciarelli. Vol. 1, p. 609. Rome, Istituto Superiore di Sanita, 1968.
55. STERIO, D. C.: The Unbiased Estimation of Number and Sizes of Arbitrary Particles Using the Disector. J. Microsc., **134:** 127-136, 1984.
56. THOMPSON, R. C., JR., and ROBINSON, H. J., JR.: Current Concepts Review. Articular Cartilage Matrix Metabolism. J. Bone and Joint Surg., **63-A:** 327-331, Feb. 1981.
57. THORNGREN, K.-G., and HANSSON, L. I.: Effect of Withdrawal of Growth Hormone Administration on Longitudinal Bone Growth in the Hypophysectomized Rat. Acta Endocrinol., **75:** 11-23, 1974.
58. THORNGREN, K.-G., and HANSSON, L. I.: Cell Production of Different Growth Plates in the Rabbit. Acta Anat., **110:** 121-127, 1981.
59. TRELSTAD, R. L., and SILVER, F. H.: Matrix Assembly. *In* Cell Biology of Extracellular Matrix, pp. 179-215. Edited by E. D. Hay. New York, Plenum Press, 1981.
60. URBAN, J. P. G.; MAROUDAS, A.; BAYLISS, M. T.; and DILLON, J.: Swelling Pressures of Proteoglycans at the Concentrations Found in Cartilaginous Tissues. Biorheology, **16:** 447-464, 1979.
61. VAES, GILBERT: I. Cellular Secretion and Tissue Breakdown. Cell-to-Cell Interactions in the Secretion of Enzymes of Connective Tissue Breakdown, Collagenase and Proteoglycan-Degrading Neutral Proteases. A Review. Agents and Actions, **10:** 474-485, 1980.
62. WALKER, K. V. R., and KEMBER, N. F.: Cell Kinetics of Growth Cartilage in the Rat Tibia. I. Measurements in Young Male Rats. Cell and Tissue Kinet., **5:** 401-408, 1972.
63. WEIBEL, E. R.: Stereological Methods. Vol. 1, pp. 245-252. London, Academic Press, 1979.
64. WONG, P. Y.-K.; MAJESKA, R. J.; and WUTHIER, R. E.: Biosynthesis and Metabolism of Prostaglandins in Chick Epiphyseal Cartilage. Prostaglandins, **14:** 839-851, 1977.